

## Characterization of nanocrystalline anatase titania: an in situ HTXRD study

Neelam Jagtap, Mahesh Bhagwat, Preeti Awati, Veda Ramaswamy\*

*Catalysis Division, National Chemical Laboratory, Pune 411008, India*

Received 18 June 2004; received in revised form 11 August 2004; accepted 12 August 2004

Available online 19 September 2004

### Abstract

Nanocrystalline titania was synthesized by the hydrolysis of titanium iso-propoxide using ultrasonication. The powder XRD patterns of the sample were recorded in static air and vacuum using a Philips X-pert Pro diffractometer equipped with a high-temperature attachment (HTK16) from room temperature (298 K) to 1173 K and were analyzed by the Rietveld refinement technique. The anatase to rutile phase transformation was observed at 1173 K for the data collected in static air. Only 3% of anatase titania transformed to rutile when the experiments were carried out at 1173 K in vacuum. The phase transformation from anatase to rutile is accompanied by a continuous increase in the crystallite size of the anatase phase from 9 nm at room temperature to 28 nm at 873 K and then to 50 nm at 1173 K in air while the process of crystallite growth was suppressed in vacuum. A linear increase in the unit cell parameters 'a' and 'c', and thus, an overall linear increase in the unit cell volume was observed as a function of temperature in static air as well as vacuum. The lattice and volume thermal expansion coefficients (TEC),  $\alpha_a$ ,  $\alpha_c$  and  $\alpha_v$  at 873 K are  $8.57 \times 10^{-6}$ ,  $8.71 \times 10^{-6}$  and  $25.91 \times 10^{-6} \text{ K}^{-1}$  in air and  $18.01 \times 10^{-6}$ ,  $14.95 \times 10^{-6}$  and  $51.13 \times 10^{-6} \text{ K}^{-1}$  in vacuum, respectively.

© 2004 Elsevier B.V. All rights reserved.

**Keywords:** Anatase; Rutile; Titania; HTXRD; Rietveld refinement; Thermal expansion coefficient

### 1. Introduction

Nanostructured titania with ultrafine crystallite sizes (<100 nm) and high surface areas have attracted substantial interest due to their unusual optical, electrical and catalytic properties [1–6]. Titania is one of the most widely used materials as a photo catalyst and finds applications in a variety of redox reactions involving various temperature/pressure conditions [7,8]. The factors that govern the photo catalytic properties of  $\text{TiO}_2$  are its phase composition and the crystallite size [9,10]. Titanium (IV) oxide exhibits three polymorphs viz., anatase, brookite and rutile. Out of these, anatase and brookite are the room-temperature phases and are transformed into the thermodynamically most stable rutile phase at higher temperature [11]. In the anatase phase,  $\text{TiO}_6$  octahedra are connected

to each other at four centers. As the temperature increases, these octahedrons dislocate increasing the strain energy of lattice, and this type of disordered lattice of anatase favors its transformation to the rutile structure [12]. Out of the three polymorphs, the anatase phase draws wide attention because of its activity as a photocatalyst [13]. Hence, the synthesis of single-phase nanocrystalline anatase titania has attained great importance in the past decade. Further, the stability of the anatase phase and the structural features of anatase titania have been the areas of strong research interest.

There have been many attempts to study the phase transformation behavior of the anatase titania as a function of particle size [12–14] and pH of the synthesis gel [15]. There are few attempts made to explain the phase transformation behavior [16] and crystal growth in nanoparticles [17] with the help of high-temperature X-ray diffraction technique using synchrotron radiation. HTXRD has been used for in situ study of the phase transformations and changes

\* Corresponding author. Tel.: +91 20 2589 3761; fax: +91 20 2589 3761.  
E-mail address: [veda@cata.ncl.res.in](mailto:veda@cata.ncl.res.in) (V. Ramaswamy).

in crystallite size with calcination temperatures by Hu et al. [18].

In the present work, we report the structural and thermal characterization of anatase titania in air and vacuum by using in situ high-temperature powder X-ray diffraction technique. The X-ray diffraction patterns obtained at various temperatures have been analyzed by the Rietveld refinement technique. The behavior of the crystallite size and the lattice parameters of the anatase phase as a function of temperature in air and vacuum are discussed.

## 2. Experimental

### 2.1. Synthesis

Titania nanocrystals were synthesized by the hydrolysis of titanium isopropoxide under ultrasonication. Titanium isopropoxide (21 mL, 0.1 mol, Aldrich) was mixed with 25 mL of absolute isopropyl alcohol. To this mixture, 29 mL of water with four drops of acetic acid were added under ultrasonication (Sheshin ultrasonicator, Japan, 100 V, 30 W, and 38 kHz). The sol gel formed was ultrasonicated for 30 min. Then, the sample was centrifuged and dried at 573 K in air to obtain nanocrystalline titania particles [6].

### 2.2. Characterization

The powder X-ray diffraction data of the  $\text{TiO}_2$  sample were obtained on a Philips X' Pert Pro diffractometer in the reflection geometry. The high-temperature experiments were carried out in static air as well as in vacuum using an Anton Paar high-temperature attachment (HTK-16). The sample was mounted on a platinum strip, which acted as the sample holder as well as the heating element. To the bottom of the platinum strip was soldered a Pt/Pt–Rh thermocouple. The data were collected in the continuous mode between the  $2\theta$  range of  $20\text{--}80^\circ$  with a step of  $0.02^\circ$  and a rate of  $2^\circ \text{min}^{-1}$ . The data were collected at temperatures ranging from 298 to 1173 K. The sample was heated at a rate of  $5 \text{ K min}^{-1}$  and a soak time of 10 min was employed at each temperature step before the scan. Si was used to calibrate the diffractometer to obtain corrected ' $d$ ' spacing.

Rietveld refinement of the powder XRD profiles was carried out using X' Pert Plus Rietveld software. The data could not be used to exploit the detailed structural information due to the poor counting statistics of the relatively fast HTXRD scan. However, the data were good enough to study the phase changes and the changes in the lattice parameters and crystallite size of the phases as a function of temperature.

## 3. Results and discussion

In situ HTXRD experiments are useful in understanding the phase stability of nanocrystalline materials. Various stud-

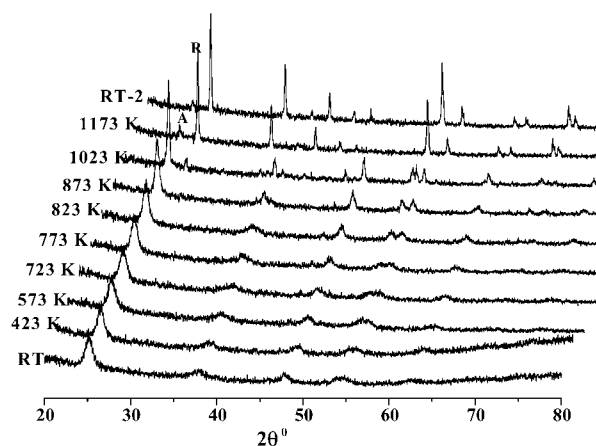


Fig. 1. The multiple plots of powder XRD patterns of the titania sample scanned in air at various temperatures from 300 to 1173 K.

ies [11,16,17] have shown that temperature–pressure phase diagrams of coarse-grained specimens [19] are no longer valid for nanomaterials. Figs. 1 and 2 show the multiple plots of the HTXRD patterns of the titania sample scanned in air and in vacuum, respectively, at various temperatures from room temperature to 1173 K and again at room temperature after cooling. The powder patterns indicate presence of anatase titania. The broad nature of the peaks indicates the nanocrystalline nature of the anatase crystals. There is no brookite phase seen at any of the temperatures studied, indicated by the absence of (1 2 1) reflection of brookite at  $2\theta = 30.81^\circ$ . Hu et al. [18] have observed increase in the concentration of brookite phase with temperature up to 923 K ( $650^\circ\text{C}$ ). The multiple plots of the powder patterns measured in static air (Fig. 1a) indicate stability of the anatase phase of titania at temperature as high as 1023 K. At temperatures higher than 1023 K, the expected anatase to rutile phase transformation can be observed. At 1173 K, almost

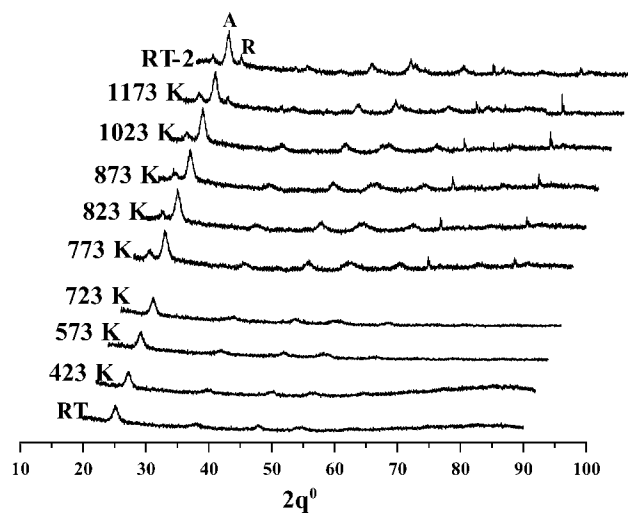


Fig. 2. The multiple plots of powder XRD patterns of the titania sample scanned in vacuum at various temperatures from 298 to 1173 K.

95% anatase phase is transformed into the rutile phase. The Bragg reflections of rutile phase are sharper than those of the anatase phase indicating higher crystallite size of the rutile phase. The powder pattern of the sample, when cooled to room temperature, is similar to the pattern at high temperature (1173 K), indicating irreversible anatase to rutile phase transformation. Nicula et al. [16] have reported the anatase to rutile transformation at 733 K (460 °C), which is roughly the half of the value reported for coarse-grained titania [19], which is ~1173 K (900 °C). The nanoparticles of anatase (~9 nm) prepared by us have higher stability (up to 1023 K) in static air, may be due to the absence of core shell (rutile-coated anatase) nanoparticles, which was observed in literature for the same crystallite size [16]. The onset temperature for the transformation of nanocrystalline anatase to rutile reported in literature [11,16–18] vary to an extent, due to the presence or absence of secondary phases viz., brookite phase, which enhances early transition temperature of anatase to rutile [15,18,20]. Absence of any traces of brookite in our samples is likely to be responsible for the better stability of anatase phase and increases the transition temperature of anatase to rutile to 1023 K (750 °C).

From the multiple plots of the XRD patterns of the sample scanned in vacuum at different temperatures given in Fig. 1b, it can be observed that the anatase phase is retained even at temperature as high as 1023 K. At 1173 K, only 3% anatase phase gets converted into the rutile phase. The anatase phase is thus more stable in vacuum than in air. This is likely to be due to the absence of atmospheric oxygen, which is used by the titania system during the phase change from anatase to rutile when the experiments are carried out in air. An additional peak is observed at  $2\theta = 23^\circ$  at 723 K and higher temperature which could be due to the contunite phase [4,5]. This peak was not observed when the experiments were carried out in air. Phases like cordierite have been reported at high pressures [21]. The change in the crystallite size with temperature is plotted in Fig. 3. The crystallite size of the anatase phase remains almost unchanged till 773 K after which the sintering of nanocrystalline anatase powder is observed, which results in the increase in the crystallite size from 9 to 50 nm when the sample was heated in air. The complete anatase to rutile transformation is accompanied by an increase in the crystal-

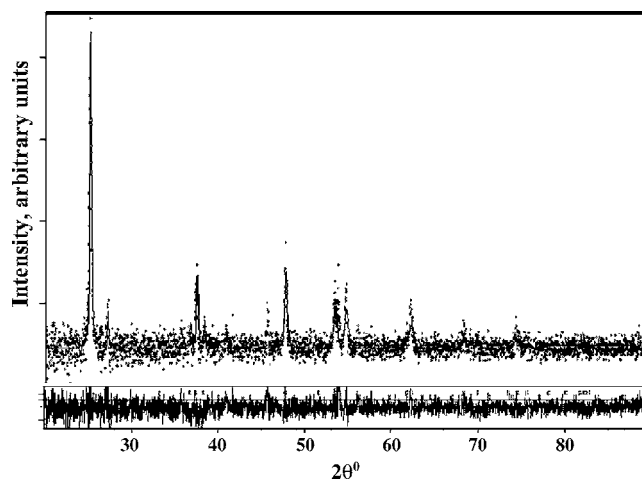


Fig. 3. The Rietveld refinement plot of the powder pattern obtained for the titania sample scanned at 1023 K in air.

lite size from 28 to 50 nm. When the sample was heated in vacuum, there was no change in the crystallite size till 773 K. On further heating, a marginal increase in the crystallite size can be seen from 9 to 12 nm till 1173 K indicating high stability of the anatase nanocrystals in vacuum.

The powder XRD patterns of the titania sample were refined by the Rietveld refinement procedure to exploit information related to the phase composition, the lattice parameters and crystallite size of the phases. The anatase phase with space group  $I4_1/amd$  and the rutile phase with space group  $P4_2/mnm$  were used as the starting models. The background in the XRD pattern was refined using a polynomial with six refinable variables. The peak shape was corrected using a Pseudo-Voigt function. The peak width (FWHM) was determined using the equation,  $FWHM = \sqrt{(U + V \tan \theta + W \tan^2 \theta)}$ , and then the crystallite size was determined using the Scherer equation,  $L = k\lambda/\beta \cos \theta$ , where  $k$  is the Scherer constant (0.9 assuming that the particles are spherical),  $\lambda = 1.5406 \text{ \AA}$  (Cu  $K\alpha$  radiation),  $\beta$  is the FWHM of sample after correcting for instrumental broadening and  $\theta$  is the angle of diffraction [22] of the strongest (1 0 1) and (1 1 0) reflections of anatase and rutile, respectively. Fig. 2 shows the observed, calculated and the difference XRD profiles of a

Table 1

Unit cell parameters of nanocrystalline anatase titania determined from the HTXRD profiles scanned in air and vacuum

Temperature (K)	In air			In vacuum		
	$a$ (Å)	$c$ (Å)	$V$ (Å <sup>3</sup> )	$a$ (Å)	$c$ (Å)	$V$ (Å <sup>3</sup> )
298	3.777 (3)	9.488 (8)	135.39	3.777 (3)	9.488 (8)	135.39
423	3.788 (1)	9.490 (2)	136.18	3.797 (2)	9.501 (2)	136.96
573	3.789 (3)	9.501 (6)	136.43	3.806 (1)	9.527 (9)	138.01
723	3.789 (5)	9.515 (9)	136.65	3.808 (5)	9.547 (3)	138.42
773	3.791 (2)	9.521 (4)	136.85	3.814 (1)	9.550 (3)	138.94
823	3.793 (7)	9.522 (4)	137.05	3.815 (5)	9.555 (3)	139.10
873	3.795 (9)	9.536 (2)	137.40	3.816 (4)	9.570 (1)	139.37
1023	–	–	–	3.821 (4)	9.576 (7)	139.85
1173	–	–	–	3.820 (8)	9.579 (7)	139.84

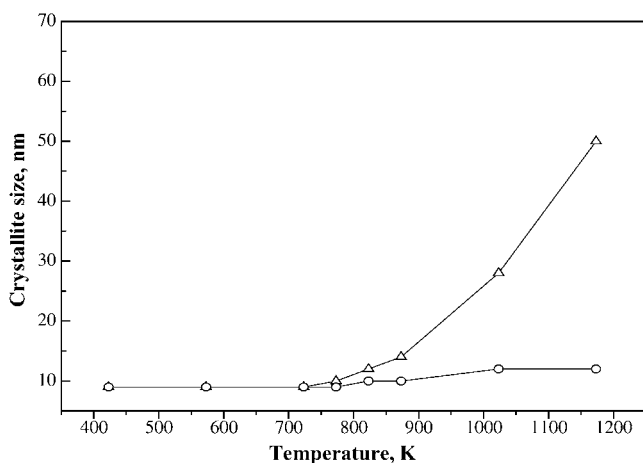


Fig. 4. The change in the crystallite size of the anatase phase with temperature. ( $\Delta$ ) = air, ( $\circ$ ) = vacuum).

typical Rietveld refinement of the titania sample scanned in air at 1023 K. In spite of a higher  $R_{\text{EXP}}$  (13.92), the goodness of fit of 1.9 indicated a good refinement of the data. The vertical ticks are indicative of Bragg reflections for the phases. The change in the lattice parameters 'a', 'c' and the unit cell volume 'V' was monitored as a function of temperature. The variation in lattice parameters 'a' and 'c' and unit cell volume  $V$  as a function of temperature is given in Table 1. There is a linear increase in  $a$ ,  $c$  and  $V$  for samples scanned in both air and vacuum. The increase is more pronounced in vacuum than in air.

The variation of % lattice thermal expansions along  $a$ : ( $\Delta a \times 100/a$ );  $c$ : ( $\Delta c \times 100/c$ ) and % volume thermal expansion  $V$ : ( $\Delta V \times 100/V$ ) with temperature are given in Figs. 4–6, respectively. There is a linear increase in the % thermal expansion in all the directions. The maximum % lattice thermal expansion observed along 'a' is 0.49% in air while the expansion is as high as 1.033% in vacuum at 873 K. The sample shows % lattice thermal expansion of 0.5% in air and 0.86%

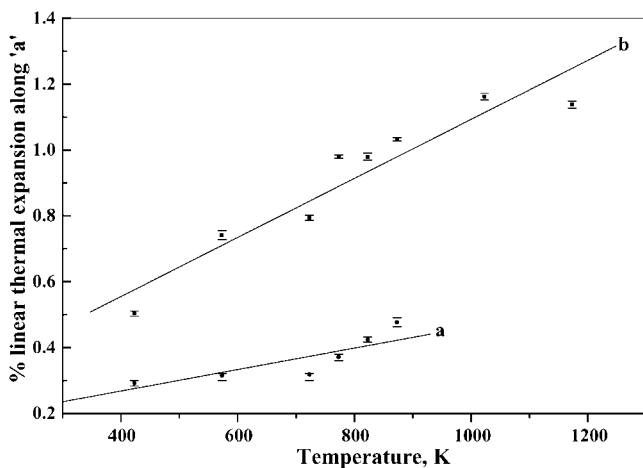


Fig. 5. The % linear thermal expansion along the 'a' axis as a function of temperature. (a = air, b = vacuum).

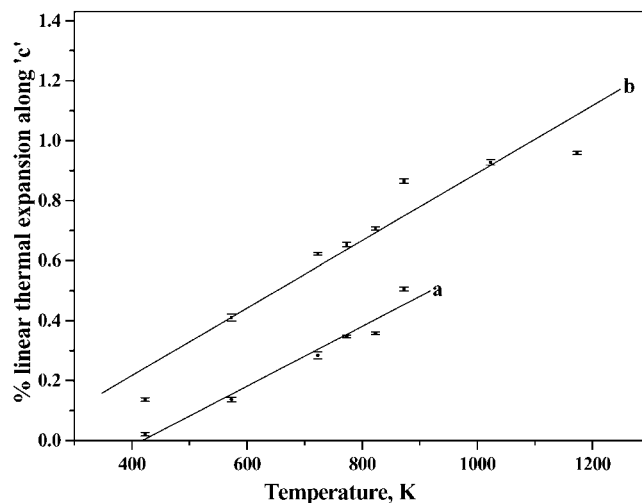


Fig. 6. The % linear thermal expansion along the 'c' axis as a function of temperature. (a = air, b = vacuum).

in vacuum along the 'c' axis. It can be observed that the % volume thermal expansion in vacuum (2.94%) is almost double than that of air (1.49%) at 873 K. A maximum of 4.45% volume expansion can be observed in vacuum at 1173 K (Fig. 7).

The thermal expansion coefficient along the 'a' and 'c' direction and the volume thermal expansion coefficients were calculated using the following equations.

$$\alpha_a = \frac{\Delta a}{(T - RT)a_{RT}}$$

$$\alpha_c = \frac{\Delta c}{(T - RT)c_{RT}}$$

$$\alpha_V = \frac{\Delta V}{(T - RT)V_{RT}}$$

where  $RT$  is the room temperature (298 K) and  $T$  is the temperature at which the measurement was done. Table 2 gives

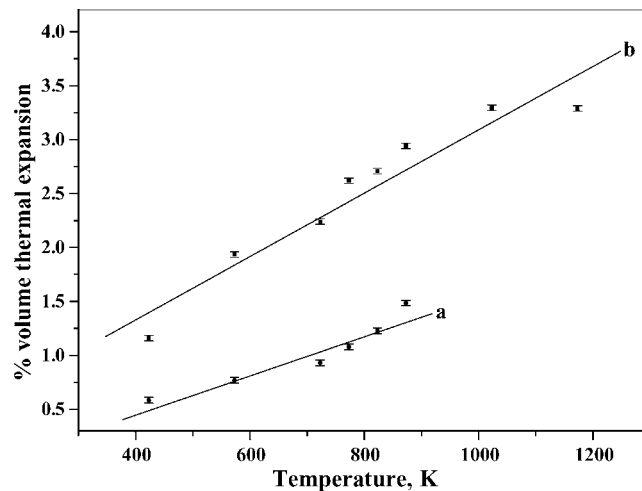


Fig. 7. The change in the % volume thermal expansion as a function of temperature. (a = air, b = vacuum).

Table 2  
Percentage of Thermal expansion coefficients of nanocrystalline anatase titania

Temperature (K)	$\alpha_a = \Delta a/(T - RT)_{aRT} \times 10^{-6} \text{ K}^{-1}$		$\alpha_c = \Delta c/(T - RT)_{cRT} \times 10^{-6} \text{ K}^{-1}$		$\alpha_V = \Delta V/(T - RT)V_{RT} \times 10^{-6} \text{ K}^{-1}$	
	Air	Vacuum	Air	Vacuum	Air	Vacuum
423	23.13	43.04	1.16	10.58	47.44	94.22
573	11.59	28.12	4.92	15.1	28.14	70.88
723	7.60	19.40	6.73	14.57	22.0	52.95
773	7.75	20.70	7.25	13.63	22.78	55.36
823	8.27	19.23	6.76	13.39	23.43	51.77
873	8.57	18.01	8.71	14.95	25.91	51.13
1023		16.25		12.81		45.56
1173		13.28		10.97		37.68

the thermal expansion coefficient along 'a' ( $\alpha_a$ ) and 'c' ( $\alpha_c$ ) and lattice thermal expansion coefficient ( $\alpha_V$ ) calculated using the above equations. The thermal expansion coefficient of  $8.57 \times 10^{-6} \text{ K}^{-1}$  was observed along the 'a' direction and  $8.71 \times 10^{-6} \text{ K}^{-1}$  along the 'c' direction in air at 873 K, whereas the thermal expansion coefficient values were higher in vacuum along 'a' ( $18.01 \times 10^{-6} \text{ K}^{-1}$ ) as well as 'c' ( $14.95 \times 10^{-6} \text{ K}^{-1}$ ) directions at 873 K. The volume thermal expansion coefficient of  $25.91 \times 10^{-6}$  and  $51.13 \times 10^{-6} \text{ K}^{-1}$  were observed for experiments carried out in air and vacuum, respectively at 873 K. The thermal expansion coefficient of titania reported in literature (brochures from different manufacturers of titania) is  $8.5 \times 10^{-6} \text{ K}^{-1}$  at 293–1273 K for 2–4  $\mu\text{m}$  coarse-grained titania. In our nanocrystalline titania sample of 9 nm, the volume thermal expansion coefficient in air is nearly three times that of coarse-grained titania.

#### 4. Conclusions

In situ HTXRD experiments of nanocrystalline anatase titania in air and vacuum are carried out to study the onset temperature for the transformation of anatase to rutile phase. Brookite phase was absent in the temperature range studied. The anatase sample showed higher stability in vacuum as compared to air atmosphere. The onset of transformation temperature for anatase in air was 1023 K, and complete transformation ( $\sim 95\%$ ) for anatase to rutile occurred at 1173 K. On the other hand, in vacuum, the transformation of anatase to rutile is suppressed due to lack of oxygen and only 3% of anatase is transformed to rutile at 1173 K. The unit cell parameters 'a' and 'c', and the unit cell volume increase linearly with increase in temperature under both the atmospheres (air and vacuum). Although the crystallite size increases with temperature in static air, the crystallite growth or the sintering effect is suppressed in vacuum. Nanocrystalline anatase titania exhibits higher % thermal expansion in vacuum than in air.

#### Acknowledgements

The authors are grateful to DST, New Delhi for financial support. One of the authors (M.B.) is thankful to CSIR, New Delhi for a fellowship.

#### References

- [1] B.J. Levy, *Electroceramics* 1 (1997) 239.
- [2] B.Y. Jian, X.P. Zhao, *Chem. Mater.* 14 (2002) 4633.
- [3] K.M. Reddy, S.V. Manorama, A.R. Reddy, *Mater. Chem. Phys.* 78 (2002) 239.
- [4] Xu, An-Wu, Gao, Yuan Liu, Han-Qin, *J. Catal.* 207 (2) (2002) 151.
- [5] H. Lachheb, E. Puzenat, A. Houas, M. Ksibi, E. Elaloui, C. Guillard, J.M. Herrmann, *Appl. Catal. B: Environ.* 39 (2002) 75.
- [6] P.S. Awati, S.V. Awate, P.P. Shah, V. Ramaswamy, *Catal. Commun.* 4 (2003) 393.
- [7] I.-H. Tseng, W.-C. Chang, C.S.W. Jerry, *Appl. Catal. B: Environ.* 37 (2002) 37.
- [8] A.V. Vorontsov, A.A. Altyinnikov, E.N. Savinov, E.N. Kurkin, *J. Photochem. Photobiol. A Chem.* 144 (2) (2001) 193.
- [9] W. Huang, Z. Tang, Y. Wang, Y. Kolytyn, A. Gedanken, *Chem. Commun.* (2000) 1415.
- [10] P. Arnal, R.J.P. Corriu, D. Leclercq, P.H. Mutin, A. Vioux, *J. Mater. Chem.* 6 (12) (1996) 1925.
- [11] H. Zhang, J.F. Banfield, *J. Phys. Chem. B* 104 (2000) 3481.
- [12] L.E. Depero, P. Bonzi, M. Zocchi, C. Casale, G. De Michele, *J. Mater. Res.* 8 (10) (1996) 2709.
- [13] L. Jong, H.N. Wooseok, K. Misook, H.G. Yong, Y.K. June, M. Ogino, K.M. Siezo, C.S. Jin, *Appl. Catal., A Gen.* 244 (1) (2003) 49.
- [14] H. Zhang, J.F. Banfield, *J. Mater. Chem.* 8 (1998) 2073.
- [15] Y. Hu, H.-L. Tsai, C.-L. Huang, *Mater. Sci. Eng. A* 344 (2003) 209.
- [16] R. Nicula, M. Stir, C. Schick, E. Burel, *Thermochim. Acta* 403 (2003) 129.
- [17] B. Gilbert, H. Zhang, F. Huang, M. Finnegan, G. Waychunas, *J. Banfield, Geochem. Trans.* 4 (2004) 20.
- [18] M. Hu, V. Kurian, E.A. Payzant, C.J. Rawn, R.D. Hunt, *Powder Technol.* 110 (2000) 2.
- [19] R.D. Shannon, J.A. Pask, *J. Am. Ceram. Soc.* 48 (1965) 391.
- [20] F. Dachille, P.Y. Simons, R. Roy, *Am. Miner.* 53 (1968) 1929.
- [21] V. Swamy, L.S. Dubrovinsky, N.A. Dubrovinskaja, A.S. Simionovici, M. Drakopoulos, V. Dmitriev, H.-P. Weber, *Solid State Commun.* 125 (2003) 111.
- [22] H.P. Klug, L.E. Alexander, *X-ray Diffraction Procedure*, 2nd ed., Wiley, New York, 1974, p. 697.